Journal of Applied Polymer Science

Nano-Dimensional Self Assembly of Regioregular Poly (3-hexylthiophene) in Toluene: Structural, Optical, and Morphological Properties

Ashish Kumar,[1] Wataru Takashima,[2] Keiichi Kaneto,[3] Rajiv Prakash[1]

[1]School of Materials Science and Technology, Indian Institute of Technology, Banaras Hindu University, Varanasi 221005, India

[2]Research Center for Advanced Eco-Fitting Technology, Kyushu Institute of Technology, 2-4 Hibikino, Wakamatsu-ku Kitakyushu 808-0196, Japan

[3]Graduate School of Life Science and Systems Engineering, Kyushu Institute of Technology, 2-4 Hibikino, Wakamatsu-ku Kitakyushu 808-0196, Japan

Correspondence to: R. Prakash (E-mail: rajivprakash12@yahoo.com)

ABSTRACT: This article presents the optimization and systematic analysis of the growth kinetics of fiber formation of the regioregular poly (3-hexylthiophene), rr-P3HT. In addition to it a comparative study of as-prepared fiber with fresh, quenched (at −7°C) and commercial rr-P3HT formed in toluene solvent. The rr-P3HT ($M_w \approx 5340$; polydispersity ≈ 1.22) is synthesized using a well known Grignard metathesis reaction and characterized by ^{1}HNMR and FTIR techniques. The films obtained by the ageing of rr-P3HT solution for 20 days contain nanostructured fiber with 6–10 nm thickness. However, it acquires a nanostructured globular shape when same concentration of solution is sudden quenched at −7°C. A saturation point for the growth of nano fiber is observed under UV–visible study and it is found that 10 days are sufficient for fiber growth. The concentration dependent free exciton band width of fiber growth is studied by Frank–Condon principle and correlated with AFM morphological studies. © 2014 Wiley Periodicals, Inc. J. Appl. Polym. Sci. **2014**, *131*, 40931.

KEYWORDS: ageing; conducting polymers; fibers; nanostructured polymers; self-assembly

Received 30 November 2013; accepted 28 April 2014

DOI: 10.1002/app.40931

INTRODUCTION

Poly (3-alkylthiophenes) is considered as one of the most excellent conjugated polymer that has potentials applications towards OFET,[1–3] photovoltaic cells,[4–7] sensor[8–10] in its pure form, as constituent in polymer blend or in composite form due to its high carrier transport on π-conjugated polythiophene chains. Moreover alkyl side chain enables them to fairly soluble in organic solvents, which is generally rare in other conjugated polymers. Poly (3-hexylthiophene), P3HT is one of the ubiquitous polymers used as a conductor in these devices due to relatively good solvation property and processibility than other polythiophens with alkyl side chain.[11–14] For the industrial point of view, the aggregation of rr-P3HT into one-dimensional nanostructures, such as nanofibers and nanowires, is a promising strategy for improving the device performance.[15,16] The nanofibers of rr-P3HT are produced by various solution-based procedures: template method,[17,18] electro-spinning,[19,20] epitaxial crystallization method,[21] copolymerization,[22] self-organization on a substrate during drying,[23] melt spinning,[24] and self organized whisker formation in a solution.[25,26] Among these, solution aging method has potential advantages from an industrial point of view due to low-cost, effortless preparation method and ease of mass production of nanofibers. In this process, the coil-to-fiber transition can be achieved by adding an appropriate proportion of good solvent in the solution and/or elevating the temperature of solution. The deriving force for this transition and ordered aggregation is often provided by either adding poor solvent or decreasing the temperature or leaving it as such for a number of days.[27–29] It is reported that rr-P3HT is generally self-assembled into lamellar form and the fiber growth occurs perpendicular to π–π stacking.[30] Though dissolution of molecules occur, extent of regioregularity, molecular weight (including polydispersity), polymer concentration in solution, crystallization temperature, cooling rate, and solvent quality (poor or good solvent) plays an important role on the

Additional Supporting Information may be found in the online version of this article.

morphology of nano-fiber[29,31–33] Moreover there are two extreme cases of aggregation namely H and J-aggregation have been reported. In most of the cases H-aggregation exhibit blue shift and J-aggregation exhibit red shift in their absorption spectra.[34] However the concept of exciton–vibrational coupling reveals an excellent signature for the distinction of these aggregates.[35] The ratio of first two vibronic peak intensities ($A' = A_{0\text{-}0}/A_{0\text{-}1}$) in the absorption spectrum decreases (corresponding to H-aggregation) and increases (corresponding to J-aggregation) with increasing excitonic coupling.[34,36,37]

Literature survey indicates that the dimensions and densities of fiber controlled by changing the solvent used and the amount of materials during crystallization 1D growth of fiber process. The nanofibers of rr-P3HT are first studied in cyclohexanone[25] and up to now produced in various pure solvents: chloroform,[38] methylene chloride,[39] p-xylene,[40] tetrahydrofuran,[41] anosole,[26] m-xylene,[42] toluene,[43] and solvent blends: dichlorobenzene and hexane,[44] chloroform and hexane,[44] anisole and chloroform,[25] chloroform and ethyl acetate.[45] However the commercial rr-P3HT of different molecular weights was used. It is well known that high the costs of commercial rr-P3HT impeded its usage as commercial devices application. Therefore its synthesis from its precursors using suitable and controlled polymerization method is one of the choices to reduce the overall cost of fabricated device. The new level of control of polymerization process, called Grignard metathesis polymerization allows for the synthesis of rr-P3HT (having high degree of regioregularity and low polydispersities, PDIs) is more demanding method after the synthesis of such polymers by Mc Cullough group.[46] The final structure of polymer and PDIs depends on the type of additives used, position of alkyl substituent, catalyst, and ligands of the catalyst.[47] Recently this method has been extended to molecular designing especially in polythiophenes.[48] Despite the successful results for the fiber formation of rr-P3HT in toluene solvent, their systematic analysis regarding the growth kinetics of the as-synthesized P3HT is not yet been explored. The major aim of this study is to suggest a fast, easy way to generate a fiber of high-quality rr-P3HT especially using low concentrated sample at room temperature. In this article we present the results of successful synthesis of rr-P3HT by Grignard metathesis polymerization method and its characterization using 1HNMR and FTIR. After that we developed a simple way to generate long P3HT nanofibrils using low concentrated rr-P3HT. Initially, the optimization of concentration of rr-P3HT for fiber formation and its growth kinetics in toluene by UV–visible spectroscopy and AFM technique is compared to quenched and fresh rr-P3HT.

EXPERIMENTAL

Materials

The 2,5-dibromo-3-hexylthiophene, t-BuMgCl and Ni(dppp)Cl_2 were obtained from Aldrich USA. Methanol, dry ether, and acetone were purchased from Wako Chemicals, Japan. All other reagents were of analytical grade.

Synthesis of rr-P3HT

The rr-P3HT (polydispersity coefficient = 1.22) was synthesized by well known modified Grignard metathesis method reported earlier[47,49] using following procedure: 1.0 g of 2,5-dibromo-3-hexylthiophene was initially dissolved in 5 mL dry THF in a nitrogen pursed 50-mL vial. A 1.4-ml t-BuMgCl (2M, in dry ether) was then added to vial using syringe and left as such for 0.5 h for complete formation Grignard monomer (GM). After that GM was further diluted by 20 mL dry THF under vigorous stirring at 300RPM. Now polymerization reaction was initiated with a suspension of Ni(dppp)Cl_2 (13.3 g in 1 mL dry THF) and left overnight for complete polymerization. The polymerization was terminated by adding 5*N* HCl and precipitated in methanol. The crude polymer was filtered and rinsed with ammonia solution to remove extent of chloride ions. Finally this crude polymer was first extracted with acetone by "Soxhlet extraction method" until the filtrate was colorless to remove oligomers or some low molecular weighted impurities. The remaining insoluble part was again extracted consequently with hexane in same manner and dried in vacuum oven with expectation of rr-P3HT having approximately $M_n = 4380$ and $M_w = 5340$ similar to the report published earlier.[50] The dried polymer was preserved in air tight vial for further characterization.

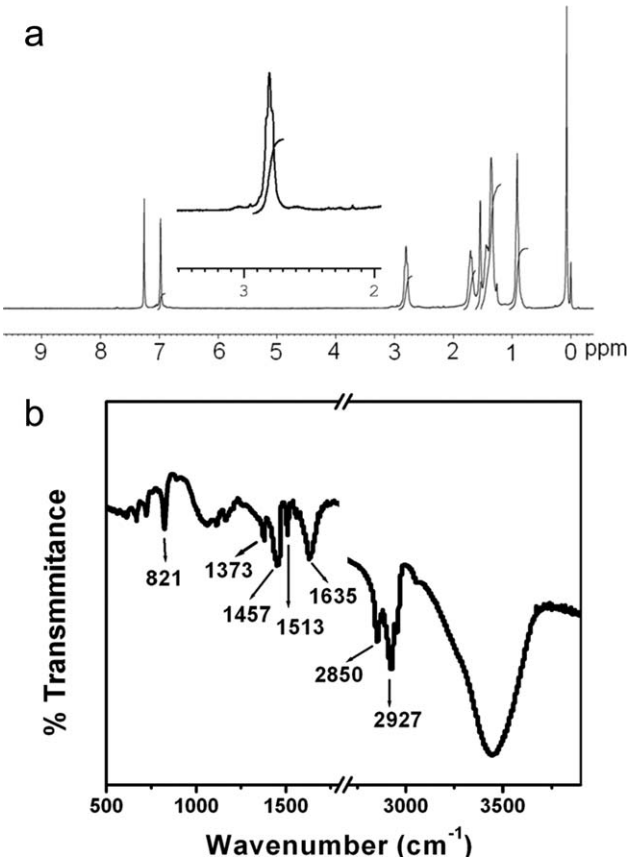

Figure 1. (a) NMR and (b) FTIR of rr-P3HT in $CDCl_3$ solvent and KBr palette respectively.

Preparation of Nanofibers and Nanoglobules

For the optimization of fiber formation 0.07, 0.05, 0.03, and 0.01% w/v rr-P3HT solution were chosen. In a typical procedure, 0.7 mg rr-P3HT was added to 1-mL toluene in a 5-mL glass vial equipped with Teflon packing, and the solution was

Table I. FTIR Band Positions (cm^{-1}) and Their Assignments of P3HT Powder

Wave numbers (cm^{-1})	Assignments
719	Methyl rocking mode
821	C—H out of phase mode
1373	Methyl deformation
1457	Symmetric C=C stretching
1513	Anti-symmetric C=C stretching
1635	Overtone of thiophene ring
2850	CH_2 out of phase vibration
2927	CH_2 in-phase vibration

dissolved by heating at 80°C. After the complete dissolution solution was gradually cooled to RT and then allowed to stand at 27°C in oven for the fiber formation. Nanofibers mainly grow in solution as time passes. Similar procedure was adopted for fiber formation by other concentrations.

For comparison purpose nanoglobules are formed by quenching method. In this procedure 0.07% rr-P3HT in toluene solvent was suddenly cooled to −7°C in ice bath for 5 min. As-synthesized rr-P3HT was characterized by NMR and FTIR prior to fiber formation or device characterization.

The ^{1}H NMR and FTIR of rr-P3HT is shown in Figure 1. In ^{1}H NMR [cf. Figure 1(a)] the presence of only one sharp band in the aromatic region ($\delta = 6.89$ ppm) as well as a clean triplet in the methylene region ($\delta = 2.5$–3.0 ppm) was indicative evidence of rr-P3HT. The expanded ^{1}H NMR spectrum in the α-methylene proton region was indicative of >96% for the regioregular linkage.[51] The rr-P3HT was further studied by FTIR spectroscopy as shown in Figure 1(b). The FTIR absorption bands are summarized in Table I which is similar to reported earlier[52,53] and presents the polymer formation.

RESULTS AND DISCUSSION

The dissolution of rr-P3HT in toluene produced a transparent orange solution at high temperatures (80°C). During cooling, the solutions displayed a dramatic color change and turned to reddish-brown after saturation of fiber formation at 27°C (shown in inset of Figure 2). The possible scenario of fiber formation is expected as follows: rr-P3HTs are in isolated state at a higher temperature due to its complete dissolution, but gradually undergo self-assemble into nanofibers at a lower temperature due to low saturating concentration similar to others.[26] Actually in this process, rr-P3HT polymers are in clustered form at room temperature (in toluene solvent), however, on elevating the temperature of the solvent, they acquires the state just before the transition of polymers from disentanglement to crystallization. Further individual unimers act as template for others to assemble together into fibrous form. These evidences were checked by UV–visible spectroscopic analysis. AFM images showed one-dimensional (1D) nanofibrillar structures on SiO_2/Si substrates where the solutions were spin coated at 3000 rpm. The fibrous rr-P3HT has the height of a few nanometers and the length of several micrometers (as discussed latter under AFM study), which represents their high aspect ratio.

Optical Properties: UV–Visible Analysis

The evolution of the UV–visible absorption spectrum with time for an isolated solution of rr-P3HT in toluene was carried out on UV/VIS/NIR spectrophotometer (Jasco V-570) that makes it possible to monitor the formation of the fibrous rr-P3HT as shown in the Figure 3. It shows the absorption spectra of a 0.07%, 0.05% rr-P3HT and a plot which is drawn in between absorbance intensity (for the peaks at 615, 570, 520, and 455 nm) and number of days for 0.07, 0.05, and 0.03% w/v solution of rr-P3HT. In this technique, the solution is heated up to 80°C to ensure the complete dissolution of the polymeric material, and is then allowed to stand at 27°C after being cooled down at room temperature. In case of 0.07% rr-P3HT [as shown in Figure 3(a)], initially only one absorbance peak at 455 nm is observed by the conjugated backbone of P3HT and remarkably, no changes are seen in the absorption spectra for the first 2 days, which indicates that the polymer chains are still well-dissolved (or entangled each other), as in a good solvent. However three consecutive shoulder peaks at 615, 570, 520 nm are observed as days passes. These shoulder peaks are actually consequences of π–π^* transition coupled to the C=C stretching in the thiophene ring,[54] while the absorbance peak at 455 nm is the well known characteristic of rr-P3HT due to π–π^* transition of isolated molecules in the solvent. The decrease in its intensity and shift toward higher wavelengths (red shift) is observed as day passes due to increase in the effective conjugation. There after this 455 nm peak merges with 520 and 570 nm peak at tenth day. At the same time three new consecutive shoulder peaks at 615 nm (after 2 days), 570 nm (after 3 days), and 520 nm (after 7 days) are also observed. Like before, these peaks also showed their shift but towards lower wavelengths. The shift of these peaks and increase in shoulder peaks (due to change in optical density) signifies the formation of crystals with face-on stacking of the planer thiophene backbone as expected.[49] It is

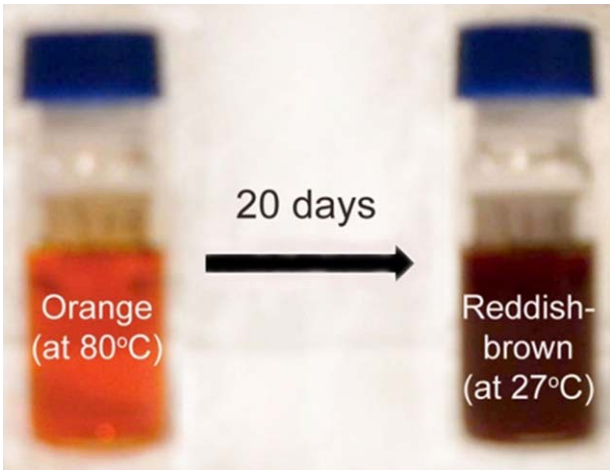

Figure 2. Photograph of a 0.07 wt % rr-P3HT solution in toluene: (left) at a high temperature (ca. 80°C) and (right) at room temperature (ca. 27°C). [Color figure can be viewed in the online issue, which is available at wileyonlinelibrary.com.]

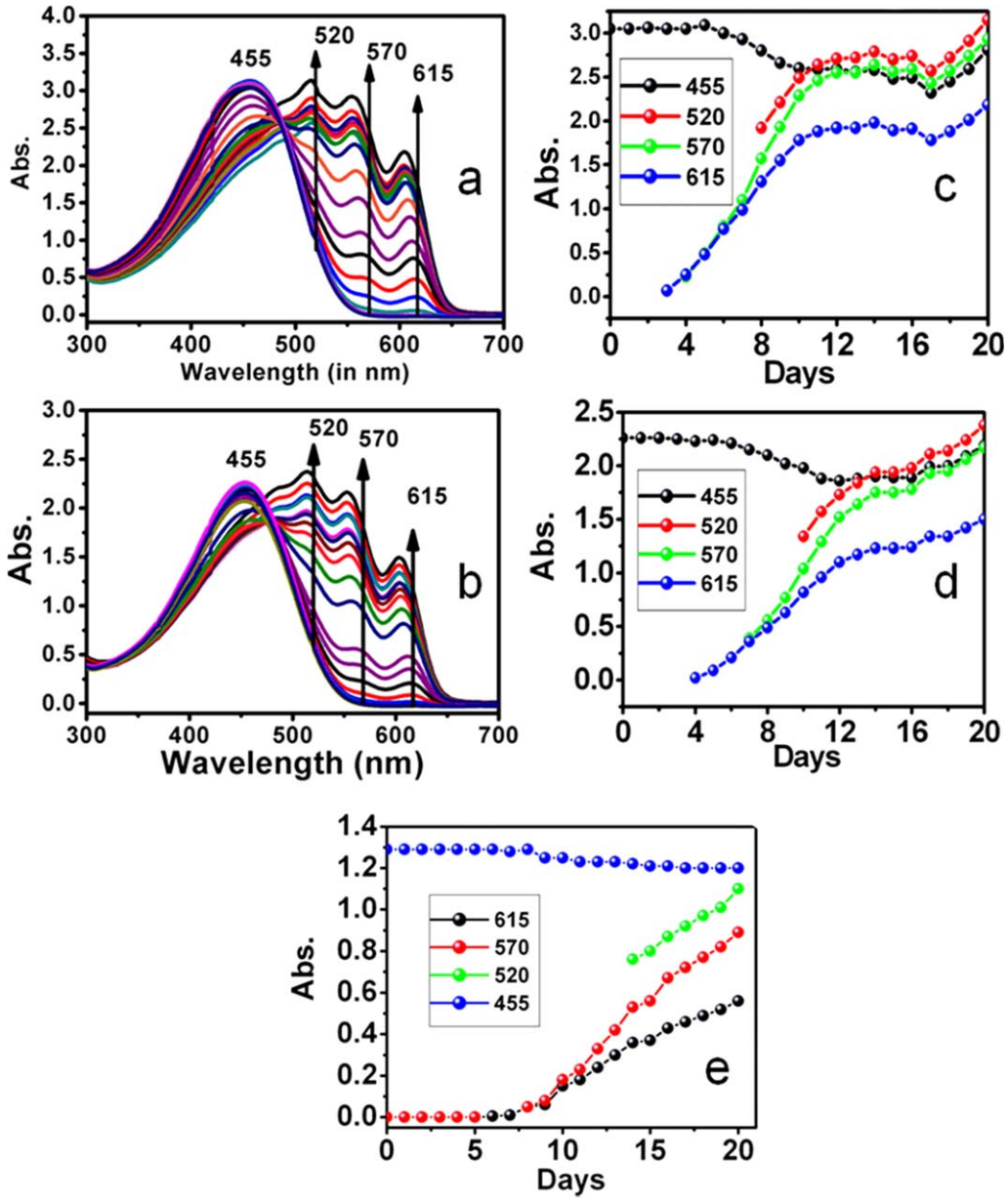

Figure 3. UV–visible spectra of (a) 0.07% rr-P3HT, (b) 0.05% rr-P3HT from 0 to 20 days and plot of absorbance verses number of day's for the peaks (at 455, 520, 570, and 615) of 0.07% (c), 0.05% (d), and 0.03% rrP3HT (e). [Color figure can be viewed in the online issue, which is available at wileyonlinelibrary.com.]

well known that the aggregation of P3HTs in this type of fashion affects opto-electrical properties on the resulted molecule[55] and crystal peak comes from the 1D P3HT structures. Because it is postulated that growth of fiber structure preferably occurs in 1D in solution and increased shoulder peaks possibly indicates the increased length of P3HT 1D nanostructures or increased number of crystals. Apart from these, the presence of single clear isosbestic point at 484 nm is another indication for transformation of isolated polymer chains directly to strongly interacting fibrous ones, without any intermediate state.[29,56] Similarly, from the calibration plot of 0.07% rr-P3HT, it is seen that the peak intensity of 615, 570, 520 peaks are constant from 10 to 17 days. Thus it is concluded that 10 day is sufficient time for fiber formation using 0.07% rr-P3HT solution. However after 17 days it is also observed that the peak intensity of 615, 570, and 520 further starts to increase. This may be probably due to curtailing of former fiber by action of gravity and formation of new fibers. Similarly for 0.05 and 0.03% rr-P3HT solution the phenomenon of fiber growth sill going on [as shown in Figure 3(d,e)] and for 0.01% solution, the chance of fiber growth is relatively few or low than other concentrations may be due to insufficient concentration for fiber growth. The fiber transformation is further justified by calculating the molar absorption coefficients (ε) change. The "ε" of isolated rr-P3HT (at 0 day) and fibrous rr-P3HT (at 20 day) are calculated from UV–vis plot for its maximum absorbance as shown in the

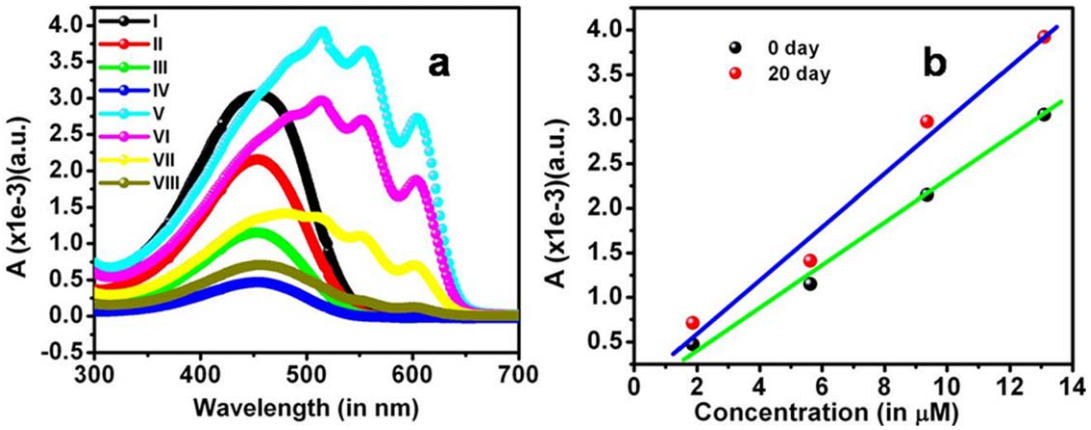

Figure 4. (a) Normalized UV–visible spectra of 0.07, 0.05, 0.03, and 0.01% rr-P3HT at 0 day (I–IV) and at 20 day (V–VIII), (b) Plot of isolated rr-P3HT (at 0 day) and fibrous rr-P3HT (at 20 day) verses concentration showing different slope. [Color figure can be viewed in the online issue, which is available at wileyonlinelibrary.com.]

Figure 4(a). It is clear that the absorption of fibrous rr-P3HT (at 20 day) is increased compared to the isolated rr-P3HT (at 0 day) and its corresponding ε (in μM^{-1} cm^{-1}) [which is obtained from slopes of Figure 4(b)] shifted about one and half times compared to that of isolated rr-P3HT (ε (fiber) = 2.99 and ε (isolated) = 2.33).

Electronic excitation in the polymer aggregates, films, and crystals are continuing to be an area of interest for a promising commercial application like solar cells, OFET, LED.[1,5,6,19,57,58] Frank–Condon principle is expected to be a good approach to explain the phenomenon of polymeric aggregations from their isolated molecular state.[34,35,59] One can derive the important information about molecular packing, the excitation band width and nature of the disorder. The absorption spectrum of aged rr-P3HT consists of two parts—a higher wavelength part (low energy) regarded as weakly interacting H-aggregates and a lower wavelength part (high energy) due to more disordered chain forming intra-chain states.[60] By the means of Gaussian fitting (for each concentrations of UV–vis curves as represented by red line fitted on the measured UV–vis plots), various possible electronic transitions are well resolved which is shown in the Figure 5 and the absorbance ratio, A′ is considered for extent of aggregation. The A′ (corresponding to the $A_{0\text{-}0}$ and $A_{0\text{-}1}$ peak absorbance) is related to the free exciton bandwidth of the aggregates, W and the energy of the main intramolecular vibration, E_p coupled to the electronic transition by the following expression as commonly used (assuming a Huang–Rhys factor of 1)[35,36]:

$$A' = (A_{0-0}/A_{0-1}) \approx \left(1 - 0.24W/E_p/1 + 0.073W/E_p\right)^2 \quad (1)$$

W is estimated using A' from Figure 5 and assuming the C=C symmetric stretching at 0.18 eV dominates the coupling to electronic transition[61] with the help of eq. (1). A decrease of W [or increase of A′ as shown in Figure 5(e)] with increase in concentration is observed which is consistent with an increase of conjugation length, reflecting fiber-like conformation.[62]

On the other hand the absorption spectrum of fibrous rr-P3HT (slow aging for 10 and 20 days) is compared with quenched rr-P3HT (fast aging) as shown in Figure 6. It is seen that the UV–visible plot of quenched rr-P3HT and fibrous rr-P3HT (aged for 10 days) have almost same absorption wavelengths at 615, 570, 520, and 455 nm but different absorption intensities [cf., Figure 6(a-I,a-II)]. Relatively high compression of 455 peak and high increment of 615, 570, and 520 peaks of fibrous

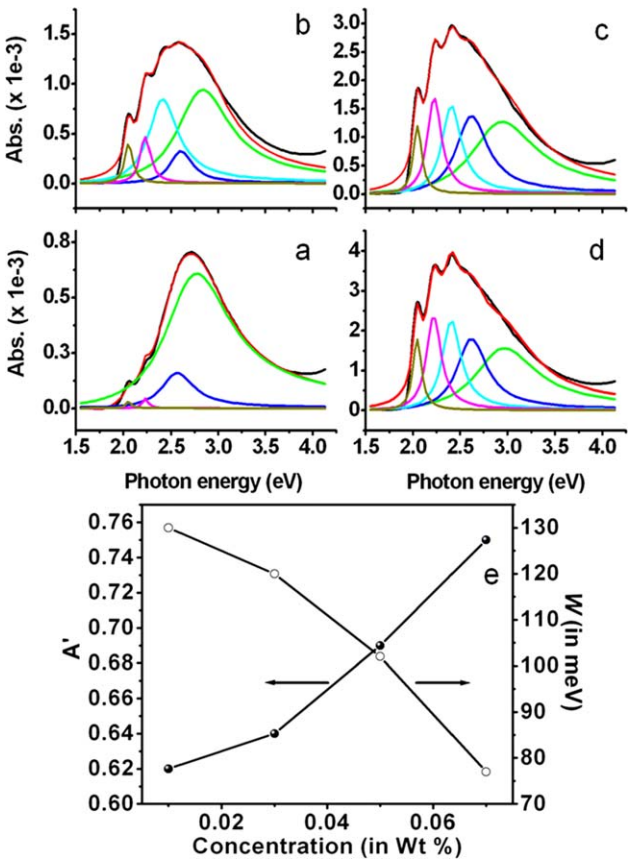

Figure 5. Gaussian fitting of normalized UV–vis plots for (a) 0.01%, (b) 0.03%, (c) 0.05%, (d) 0.07% rr-P3HT and (e) Plot of absorption ratio, A′ vs. concentration, where $A' = A_{0\text{-}0}/A_{0\text{-}1}$. [Color figure can be viewed in the online issue, which is available at wileyonlinelibrary.com.]

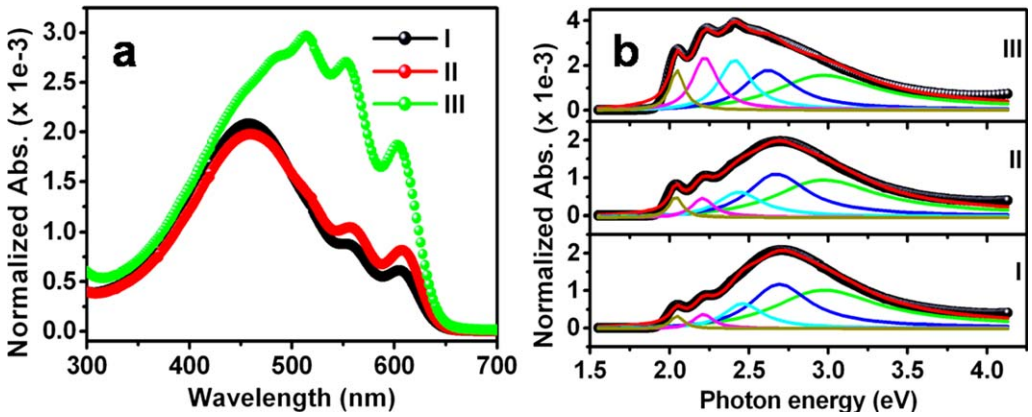

Figure 6. (a) Normalized and (b) Gaussian fitted UV–visible spectra of 0.07% (I) quenched, (II) 10 day aged and (III) 20 day aged rr-P3HT. [Color figure can be viewed in the online issue, which is available at wileyonlinelibrary.com.]

rr-P3HT compared to quenched rr-P3HT are probably due to difference in optical density causing aggregation of rrP3HT in different fashions with unique morphology (as discussed latter in AFM analysis). However these peaks shifted (as already discussed earlier) on increasing the aging time [cf., Figure 6(a-III)].

The plausible explanation for difference in morphology is as follows: In the case of slower aging process, the isolated molecules have much more time to rearrange themselves (chain folding due to self-seeding process) into a conducting domain compared to fast aging (quenching) process. In other words, we can say that polymer chains may not have enough time to disentangle prior to crystallization on rapid cooling and hence random chain folding causes different morphology.[63] Furthermore all absorption peaks are fitted in order to get the comparison of *W* [as shown in Figure 6(b)]. The value of *W* for quenched rr-P3HT (=96 meV) is observed higher than that of aged rr-P3HT (=71 meV for 10 day aged and 77 meV for 20 day aged) for the same concentration of samples. These observations

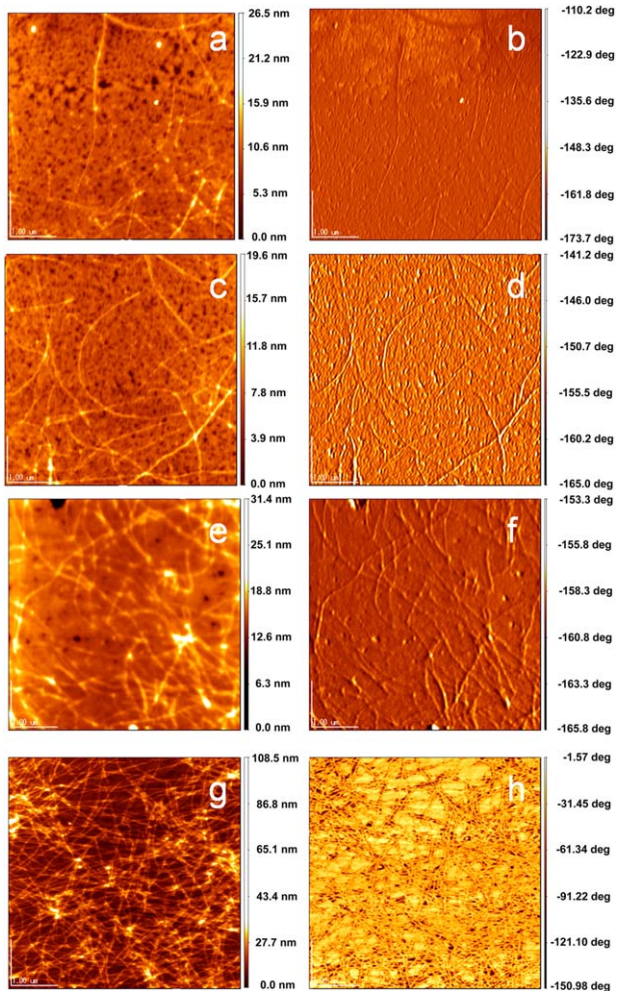

Figure 7. AFM images of 0.01, 0.03, 0.05, and 0.07% rr-P3HT; (a), (c), (e), and (g) with their corresponding phase imaging; (b), (d), (f), and (h) respectively. [Color figure can be viewed in the online issue, which is available at wileyonlinelibrary.com.]

Table II. Average Roughness Calculated from AFM of Different Samples Casted on SiO_2

rr-P3HT sample	Average roughness (in nm)
0.01% aged	0.74
0.03% aged	0.82
0.05% aged	0.96
0.07% aged	4.05
0.07% quenched (0 h)	0.70
0.07% quenched (24 h)	0.91

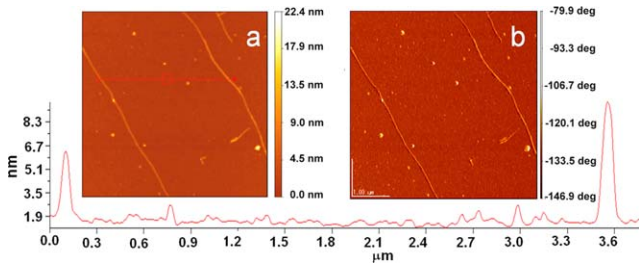

Figure 8. AFM of single fibrous rr-P3HT with their corresponding topographic and phase imaging and height profile. [Color figure can be viewed in the online issue, which is available at wileyonlinelibrary.com.]

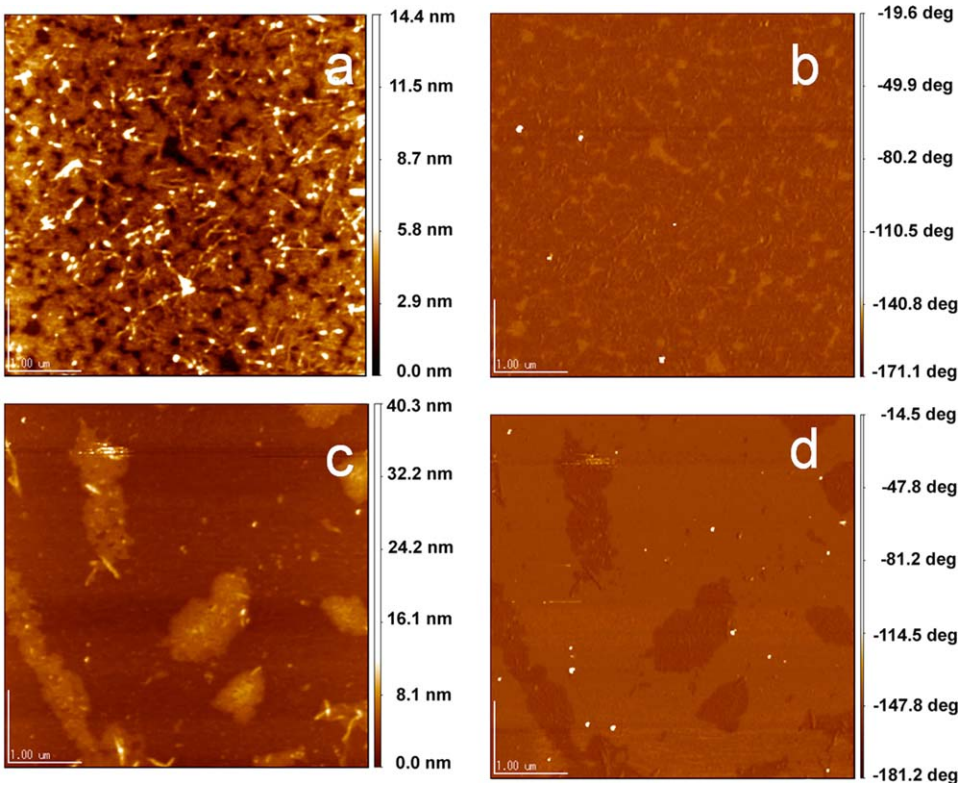

Figure 9. AFM of globular rr-P3HT (just after quenching) and irregular collapsed rr-P3HT (after 24 h); (a) and (c) with their corresponding phase imaging; (b) and (d) at −7°C respectively. [Color figure can be viewed in the online issue, which is available at wileyonlinelibrary.com.]

exemplify that the extent of conjugation (due to aggregation) is lower in case of quenched rr-P3HT. Similarly the mode of aggregation property of as-synthesized rr-P3HT and commercial rr-P3HT is compared under similar experimental conditions (as discussed in Supporting Information; Figure S1). Herein, it is observed that the extent of aggregation in both the samples is almost similar except the texture of their morphology.

Morphological Properties: AFM Study

The fibrous morphology is the signature of crystalline ordering of individual chains (as evident from UV–vis analysis also) through π-stacking with the backbone axis perpendicular to the fiberil axis (that is stacking direction) as commonly observed.[30,64] The substantial differences in morphology of all concentration of rr-P3HTs were demonstrated using AFM (JEOL-JSPM/5200, Japan) by tapping and phase imaging mode on spin casted over SiO_2/Si substrate as shown in Figure 7. The AFM images show that the fiber-like aggregation which is clearly resolved in both the topography and phase signals across the entire area as concentration increases. The dark area of phase image corresponds to depression in the film. It is clear that the progress of aggregation is lower in case of 0.01% solution compared to 0.07% solution. The isolated rr-P3HT are already exists in coiled state at lower concentration while dense fiber-like aggregation exists in higher concentration. Similarly their average roughness goes on increasing as the concentration increases (as shown in Table II). Moreover the fibrous rr-P3HT (formed by aging of 0.07% rr-P3HT solution) has a one-dimensional nanofiberillar structure with ~6–10 nm of its size [cf., Figure 8(a,b) with their height profile], which are heterogeneously distributed on the substrate [as shown as tapping and phase imaging in Figure 7(g,h)]. However in quenched rr-P3HT, all isolated polymer chains are coiled together into globular form [as shown in Figure 9(a,b)] and these small globules are collapsed together in irregular manner with slightly increase in average roughness (cf., from Table II) whenever quenched sample is left for 24 h at −7°C [as shown in Figure 9(c,d)].

CONCLUSION

In this work, rr-P3HT with polydispersity coefficient = 1.22 is synthesized successfully by well versed synthesis method. As-synthesized rr-P3HT is studied for optimization of their nanofiber formation by aging process in poor solvent (toluene) and compared with quenched and commercial rr-P3HT. The change in molar extinction coefficient from 2.33 to 2.99 μM^{-1} cm^{-1} and free exciton bandwidth from 130 to 77 meV are observed due to well known H-aggregates of rr-P3HTs in the toluene solvent. However low aggregation of isolated rr-P3HT is seen compared to aged rr-P3HT (for 10 or 20 day). We observed that 10 days is sufficient for the formation of nanofiber. Well resolved long fibrous texture having nanometric thickness (6–10 nm) with relatively excellent film with average roughness (4.05 nm) is observed for 0.07% aged rr-P3HT. Such type of effortless strategy for fibrous polymer film formation can be extended for other polymers and also may be explored for various applications such as sensors, drug- delivery, and electronic applications.

ACKNOWLEDGMENTS

The authors thank Department of Science and Technology (DST), New Delhi and Japan Society for the Promotion of Science (JSPS), Japan for the financial support under the DST-JSPS collaborative research work.

REFERENCES

1. Saito, Y.; Sakai, Y.; Higashihara, T.; Ueda, M. *RSC Adv.* **2012**, *22*, 1285.
2. Lee, H. S.; Cho, J. H.; Cho, K.; Park, Y. D. *J. Phys. Chem. C* **2013**, *117*, 11764.
3. Chang, M.; Choi, D.; Fu, B.; Reichmanis, E. *ACS Nano* **2013**, *7*, 5402.
4. Bertho, S.; Campo, B.; Piersimoni, F.; Spoltore, D.; D'Haen, J.; Lutsen, L.; Maes, W.; Vanderzande, D.; Manca, J. *Sol. Energ. Mater. Sol. C.* **2013**, *110*, 69.
5. Wu, J.; Yue, G.; Xiao, Y.; Lin, J.; Huang, M.; Lan, Z.; Tang, Q.; Huang, Y.; Fan, L.; Yin, S.; Sato, T. *Sci. Rep.* **2013**, *3*, 1.
6. Lobez, J. M.; Andrew, T. L.; Bulovic, V.; Swager, T. M. *ACS Nano* **2012**, *6*, 3044.
7. Yang, L.; Sontag, S. K.; LaJoie, T. W.; Li, W.; Huddleston, N. E.; Locklin, J.; You, W. *Appl. Mater. Interfaces* **2012**, *4*, 5069.
8. Lin, P.; Yan, F. *Adv. Mater.* **2012**, *24*, 34.
9. Dudhe, R. S.; Sinha, J.; Sutar, D. S.; Kumar, A.; Rao, V. R. *Sensor. Actuat. A Phys.* **2011**, *171*, 12.
10. Li, H.; Li, J.; Xu, Q.; Hu, X. *Anal. Chem.* **2011**, *83*, 9681.
11. Miyajima, S.; Nagamatsu, S.; Pandey, S. S.; Hayase, S.; Kaneto, K.; Takashima, W. *Appl. Phys. Lett.* **2012**, *101*, 193305.
12. Sun, Z.; Li, J.; Yan, F. *J. Mater. Chem.* **2012**, *22*, 21673.
13. Tiwari, S.; Singh, A. K.; Joshi, L.; Chakrabarti, P.; Takashima, W.; Kaneto, K.; Prakash, R. *Sensor. Actuat. B Chem.* **2012**, *171*, 962.
14. Das, S. K.; Abe, K.; Yoshino, K.; Ogomi, Y.; Pandey, S. S.; Hayase, S. *Thin Solid Films* **2013**, *536*, 302.
15. Lu, G.; Blakesley, J.; Himmelberger, S.; Pingel, P.; Frisch, J.; Lieberwirth, I.; Salzmann, I.; Oehzely, M.; Pietro, R. D.; Salleo, A.; Koch, N.; Neher, D. *Nat. Commun.* **2013**, *4*, 1588.
16. Fanous, J.; Schweizer, M.; Schawaller, D.; Buchmeiser, M. R. *Macromol. Mater. Eng.* **2012**, *297*, 123.
17. Kim, F. S.; Jenekhe, S. A. *Macromolecules* **2012**, *45*, 7514.
18. Martín, J.; Nogales, A. Martín-Gonzalez, M. *Macromolecules* **2013**, *46*, 1477.
19. Chan, K. H. K.; Yamao, T.; Kotaki, M.; Hotta, S. *Synth. Met.* **2012**, *160*, 2587.
20. Lee, S. W.; Lee, H. J.; Choi, J. H.; Koh, W. G.; Myoung, J. M.; Hur, J. H.; Park, J. J.; Cho, J. H.; Jeong, U. *Nano Lett.* **2009**, *10*, 347.
21. Brinkmann, M.; Chandezon, F.; Pansu, R. B.; Rabant, C. J. *Adv. Funct. Mater.* **2009**, *19*, 2759.
22. Geyther, J.; Gilroy, J. B.; Rupar, P. A.; Lunn, D. J.; Kynaston, E.; Patra, S. K.; Whittell, G. R.; Winnik, M. A.; Manners, I. *Eur. J.* **2013**, *19*, 9186.
23. Tu, D.; Pagliara, S.; Camposeo, A.; Potente, G.; Mele, E.; Cingolani, R.; Pisignano, D. *Adv. Funct. Mater.* **2011**, *21*, 1140.
24. Fanous, J.; Schweizer, M.; Schawaller, D.; Buchmeiser, M. R. *Macromol. Mater. Eng.* **2012**, *297*, 123.
25. Ihn, K. J.; Moulton, J.; Smith, P. *J. Polym. Sci. B Polym. Phys.* **1993**, *31*, 735.
26. Samitsu, S.; Shimomura, T.; Heike, S.; Hashizume, T.; Ito, K. *Macromolecules* **2008**, *41*, 8000.
27. Bielecka, U.; Lutsyk, P.; Janus, K.; Sworakowski, J.; Bartkowiak, W. *Org. Electron.* **2011**, *12*, 1768.
28. Xu, W.; Li, L.; Tang, H.; Li, H.; Zhao, X.; Yang, X. *J. Phys. Chem. B* **2011**, *115*, 6412.
29. Sun, S.; Salim, T.; Wong, L. H.; Foo, Y. L.; Boey, F.; Lam, Y. M. *J. Mater. Chem.* **2011**, *21*, 377.
30. Liu, J.; Sun, Y.; Gao, X.; Xing, R.; Zheng, L.; Wu, S.; Geng, Y.; Han, Y. *Langmuir* **2011**, *27*, 4212.
31. Nagarjuna, G.; Baghgar, M.; Labastide, J. A.; Algaier, D. D.; Barnes, M. D.; Venkataraman, D. *ACS Nano* **2012**, *6*, 10750.
32. Brinkmann, M.; Rannou, P. *Adv. Funct. Mater.* **2007**, *17*, 101.
33. Gilroy, J. B.; Lunn, D. J.; Patra, S. K.; Whittell, G. R.; Winnik, M. A.; Manners, I. *Macromolecules* **2012**, *45*, 5806.
34. Spano, F. C. *Acc. Chem. Res.* **2010**, *43*, 429.
35. Spano, F. C. *J. Chem. Phys.* **2005**, *122*, 234701.
36. Clark, J.; Silva, C.; Friend, R. H.; Spano, F. C. *Phys. Rev. Lett.* **2007**, *98*, 206406.
37. Spano, F. C.; Clark, J.; Silva, C.; Friend, R. H. *J. Chem. Phys.* **2009**, *130*, 074904.
38. Guo, Y.; Jianq, L.; Ma, X.; Hu, W.; Su, Z. *Polym. Chem.* **2013**, *4*, 4308.
39. Yang, H.; LeFevre, S. W.; Ryu, C. Y.; Bao, Z. *Appl. Phys. Lett.* **2007**, *90*, 172116.
40. Chen, C. Y.; Chan, S. H.; Li, J. Y.; Wu, K. H.; Chen, H. L.; Chen, J. H.; Huang, W. Y.; Chen, S. A. *Macromolecules* **2010**, *43*, 7305.
41. Huang, Y.; Cheng, H.; Han, C. C. *Macromolecules* **2011**, *44*, 5020.
42. Oh, J. Y.; Shin, M.; Lee, T. I.; Jang, W. S.; Min, Y.; Myoung, J. M.; Baik, H. K.; Jeong, U. *Macromolecules* **2012**, *45*, 7504.
43. Xue, L.; Gao, X.; Zhao, K.; Liu, L.; Yu, X.; Han, Y. *Nanotechnology* **2010**, *21*, 145303.
44. Li, L.; Lu, G.; Yang, X. *J. Mater. Chem.* **2008**, *18*, 1984.
45. Scharsich, C.; Lohwasser, R. H.; Sommer, M.; Asawapirom, U.; Scherf, U.; Thelakkat, M.; Neher, D.; Kohler, A. *J. Polym. Sci. Polym. Phys.* **2012**, *50*, 442.
46. Loewe, R. S.; Ewbank, P. C.; Liu, J.; Zhai, L.; McCullough, R. D. *Macromolecules* **2001**, *34*, 4324.
47. Jeffries-El, M.; Sauvé, G.; McCullough, R. D. *Macromolecules* **2005**, *38*, 10346.
48. Osaka, I.; McCullough, R. D. *Acc. Chem. Res.* **2008**, *41*, 1202.
49. Lohwasser, H. R.; Thelakkat, M. *Macromolecules* **2011**, *44*, 3388.

50. Trznadel, M. *Macromolecules* **1998**, *31*, 5051.
51. Kim, S. H.; Kim, J. G. *Bull. Korean Chem. Soc.* **2010**, *31*, 193.
52. Motaung, D. E.; Malgas, G. F.; Arendse, C. J.; Mavundla, S. E.; Knoesen, D. *Mater. Chem. Phys.* **2009**, *116*, 279.
53. Abdou, M. S. A.; Holdcroft, S. *Macromolecules* **1993**, *26*, 2954.
54. Sundberg, M.; Inganas, O.; Stafstrom, S.; Gustafsson, G.; Sjogren, B. *Solid State Commun.* **1989**, *71*, 435.
55. Daring, S. B. *J. Phys. Chem. B* **2008**, *112*, 8891.
56. Zhao, K.; Xue, L.; Liu, J.; Gao, X.; Wu, S.; Han, Y.; Geng, Y. *Langmuir* **2009**, *26*, 471.
57. Yuan, W. Z.; Gong, Y.; Chen, S.; Shen, X. Y.; Lam, J. W. Y.; Lu, P.; Lu, Y.; Wang, Z.; Hu, R.; Xie, H.; Kwok, H. S.; Zhang, Y.; Sun, J. Z.; Tang, B. Z. *Chem. Mater.* **2012**, *24*, 1518.
58. Park, Y. I.; Kuo, C. Y.; Martinez, J. S.; Park, Y. S.; Postupna, O.; Zhugayevych, A.; Kim, S.; Park, J.; Tretiak, S.; Wang, H. L. *Appl. Mater. Interfaces* **2013**, *5*, 4685.
59. Danesh, C. D.; Starkweather, N. S.; Zhang, S. *J. Phys. Chem. B* **2012**, *116*, 12887.
60. Wang, H.; Liu, J.; Xu, Y.; Han, Y. *J. Phys. Chem. B* **2013**, *117*, 5996.
61. Louarn, G.; Trznadel, M.; Buisson, J. P.; Laska, J.; Pron, A.; Lapkowski, M.; Lefrant, S. *J. Phys. Chem.* **1996**, *100*, 12532.
62. Barford, W. *J. Chem. Phys.* **2007**, *126*, 134905.
63. Vakhshouri, K.; Gomez, E. D. *Macromol. Rapid Commun.* **2012**, *33*, 2133.
64. Lim, J. A.; Liu, F.; Ferdous, S.; Muthukumar, M.; Briseno, A. L. *Mater. Today*, **2010**, *13*, 14.